NANO LETTERS

pubs.acs.org/NanoLett Letter

Universal Inverse Scaling of Exciton−Exciton Annihilation Coefficient with Exciton Lifetime

Shiekh Zia Uddin, Eran Rabani, and Ali Javey*

Cite This: https://dx.doi.org/10.1021/acs.nanolett.0c03820 Read Online

ACCESS | Metrics & More | Article Recommendations | Supporting Information

ABSTRACT: Be it for essential everyday applications such as bright light-emitting devices or to achieve Bose−Einstein condensation, materials in which high densities of excitons recombine radiatively are crucially important. However, in all excitonic materials, exciton−exciton annihilation (EEA) becomes the dominant loss mechanism at high densities. Typically, a macroscopic parameter named EEA coefficient (C_{EEA}) is used to compare EEA rates between materials at the same density; higher C_{EEA} implies higher EEA rate. Here, we find that the reported values of C_{EEA} for 140 different materials is inversely related to the single-exciton lifetime. Since during EEA one exciton must relax to ground state, C_{EEA} is proportional to the single-exciton recombination rate. This leads to the counterintuitive observation that the exciton density at which EEA starts to dominate is higher in a material with larger C_{EEA}. These results broaden our understanding of EEA across different material systems and provide a vantage point for future excitonic materials and devices.

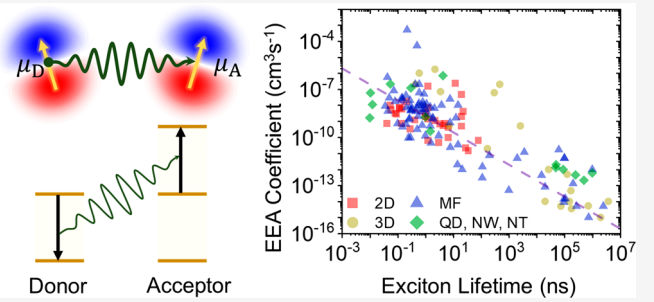

KEYWORDS: *exciton, exciton−exciton annihilation, quantum yield, photoluminescence, nonradiative recombination, universal trend*

Excitons can be formed by direct photoexcitation or by association of free electrons and holes due to their attractive Coulombic interaction. Excitons dominate the photophysics of many different classes of material systems; from nanoscale complexes[1] such as molecules,[2] molecular aggregates,[2] quantum dots,[3] nanotubes,[4] and two-dimensional semiconductors[5] at room temperature to bulk semiconductors[6] at cryogenic temperatures. At low exciton densities, many of these excitonic materials have high luminescence efficiency and this property has been leveraged in commercial light-emitting device technologies.[7] However, at high exciton concentrations the recombination is dominated by exciton−exciton annihilation (EEA), where an exciton nonradiatively recombines in the course of colliding with another exciton.[8] This nonradiative process drastically reduces the luminesce efficiency and is the leading efficiency-limiting factor in numerous applications. Although EEA is ubiquitously observed and extensively studied in excitonic materials, a clear and systematic comparison of EEA rate across different materials systems is lacking. Generally, EEA is characterized by a macroscopic parameter named exciton−exciton annihilation coefficient C_{EEA}. High values of C_{EEA} implies high EEA rates for a given exciton density.

Here, we investigate EEA across 140 different material systems (see Table S1) collected from published literature. They represent different classes of materials, such as two-dimensional (2D) and bulk semiconductors, chloroplasts, solid phase of noble gas atoms, crystalline ionic compounds, scintillators, molecular crystals and films, fluorophores, covalent organic frameworks, quantum dots array, nanotubes and nanowires, thus providing a broad basis for characterizing general patterns in EEA. The observed values of EEA coefficient and exciton lifetime in these materials spans 10 orders of magnitude. We find that across different material systems, contrary to intuition, EEA coefficient C_{EEA} is linearly correlated with the single-exciton lifetime τ_X. We explain the observed trend with a microscopic quantum theory of EEA. This trend sets a universal limiting exciton concentration of ~1 × 10^{20} cm^{-3} at which EEA starts to dominate single-exciton recombination in different materials, despite having drastically different EEA coefficients. More importantly, this trend shows that the recombination rate at the onset of EEA is linearly correlated to EEA coefficient, which is a paradigm shifting insight. These results advance our ability to recognize existing materials that can support large densities of excitons without compromising luminescence efficiency, provide a point of reference against which new materials can be benchmarked, and shed new light on the microscopic mechanism of exciton−exciton annihilation.

Received: September 21, 2020
Revised: December 10, 2020

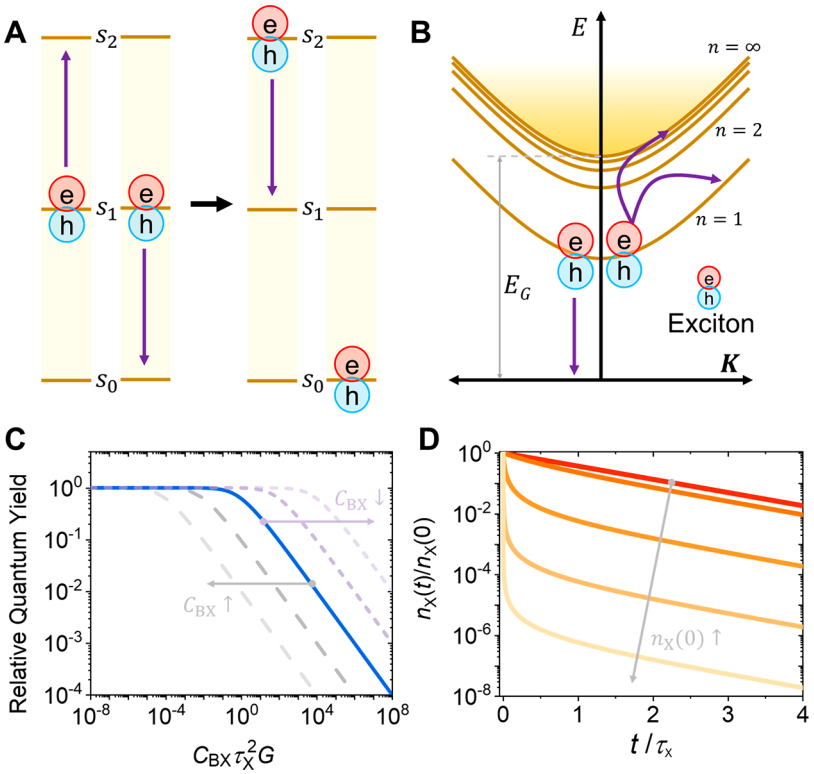

Figure 1. Mechanism and Signatures of Exciton−exciton annihilation. Schematic representation of the EEA process in (A) adjacent discrete molecules and (B) crystalline semiconductors with energy dispersion. Effect of EEA on (C) quantum yield measured by continuous excitation and (D) time-resolved exciton concentration following pulsed excitation.

Exciton, a bound state of an electron and a hole due to their attractive electrostatic Coulomb force, is often discussed in the two limiting cases depending of the size of the exciton.[1] Small Frenkel excitons have similar size as lattice spacing and are typically found in organic molecular crystals,[9] whereas Wannier−Mott excitons are larger than lattice spacing and are typically found in inorganic crystals.[10] Both types of excitons show EEA at high densities. Energy level diagram demonstrating EEA of localized Frenkel excitons with discrete energy levels are shown in Figure 1A. Initially two molecules are in their first excited state, where they each have one exciton. EEA occurs when the exciton in the right molecule moves to the ground state and sends the exciton in the left molecule to a higher energy state through energy transfer. Internal conversion by phonon emission leads to a rapid relaxation of the left molecule into its first excited state, leaving only one exciton after EEA. The energy of large and mobile Wannier-Mott excitons in semiconductor crystals depends on their center-of-mass momentum. Schematic representation of EEA for Wannier−Mott excitons along with their energy dispersion is shown in Figure 1B, where one exciton nonradiatively transfers its energy to ionize and/or increase the center-of-mass kinetic energy of another nearby exciton, conserving total momentum.

The two principal evidence that identify EEA are that (i) the luminescence quantum yield decreases sublinearly with increasing excitation power and (ii) the observed lifetime of excitons shortens substantially at high exciton densities.[11] For both Frankel and Wannier−Mott excitons, the experimental observations can be captured by a phenomenological macroscopic rate equation[12] for the exciton density $n_X(r, t)$ containing an annihilation term proportional to the square of this density

$$\frac{\partial n_X(r,t)}{\partial t} = G(r,t) + D\nabla^2 n_X(r,t) - \frac{n_X(r,t)}{\tau_X} - C_{EEA} n_X^2(r,t) \quad (1)$$

where r is position, t is time, $G(r, t)$ is the exciton generation rate, D is the exciton diffusion coefficient, τ_X is the single-exciton lifetime, and C_{EEA} is the EEA coefficient. In the case of spatially uniform generation $G(r, t) = G(t)$, the diffusion term vanishes, and eq 1 simplifies to

$$\frac{\partial n_X(t)}{\partial t} = G(t) - \frac{n_X(t)}{\tau_X} - C_{EEA} n_X^2(t) \quad (2)$$

which is widely used to describe photophysics of excitonic systems. In the case of steady-state excitation, the time derivative vanishes and $G(t) = G = \frac{n_X}{\tau_X} + C_{EEA} n_X^2$. The radiative recombination of rate is proportional to the exciton concentration. Therefore, the relative quantum yield (QY) can be written as

$$QY \propto \frac{n_X}{G} = \frac{n_X}{\frac{n_X}{\tau_X} + C_{EEA} n_X^2}$$

which is constant at low exciton density and decreases with increasing exciton density. This is one of the primary evidence of EEA (Figure 1C). We define the exciton density and generation rate, at which relative quantum yield drops to half of the low pump value, as the onset exciton density and onset recombination rate

https://dx.doi.org/10.1021/acs.nanolett.0c03820
Nano Lett. XXXX, XXX, XXX−XXX

$$n_{1/2} = \frac{1}{C_{EEA}\tau_X}, G_{1/2} = \frac{2}{C_{EEA}\tau_X^2} \quad (3)$$

For the same lifetime the onset exciton concentration decreases with increasing C_{EEA} (Figure 1C). In the case of pulsed excitation, $G(t) = n_X(0)\,\delta(t)$, where $\delta(t)$ is the Dirac delta function, time varying exciton concentration from eq 2 can be written as

$$n_X(t) = \frac{n_X(0)\exp\left(-\frac{t}{\tau_X}\right)}{1 + n_X(0)C_{EEA}\tau_X\left[1 - \exp\left(-\frac{t}{\tau_X}\right)\right]}$$

We note, at increased exciton concentration, the initial decay of the excitation population becomes faster, leading to an observation of reduced effective lifetime. This is more primary evidence of EEA (Figure 1D).

EEA has been extensively studied in many different material systems. EEA coefficient (C_{EEA}) as a function of exciton lifetime (τ_X) for different materials along with their relative histograms are shown in Figure 2. To be present in our data, a material must have been characterized in literature either by experimental techniques that track time-resolved exciton density after pulsed excitation or by steady-state measurement of luminescence efficiency as a function of exciton density. The observed values of τ_X and C_{EEA} in nature spans 10 orders of magnitude. We note from the histogram that, 2D semiconductors have relatively short exciton lifetime (0.1−10 ns), but large EEA coefficient (1×10^{-10} to 1×10^{-7} cm^3/s). In contrast, bulk semiconductors exhibit a relatively long exciton lifetime (1×10^4 to 1×10^7 ns) but a small EEA coefficient (1×10^{-15} to 1×10^{-12} cm^3/s). Molecular films, however, cover the entire range of lifetime and EEA coefficient. Over the whole range, we observe a general trend of decreasing C_{EEA} with increasing exciton lifetime τ_X for all material classes.

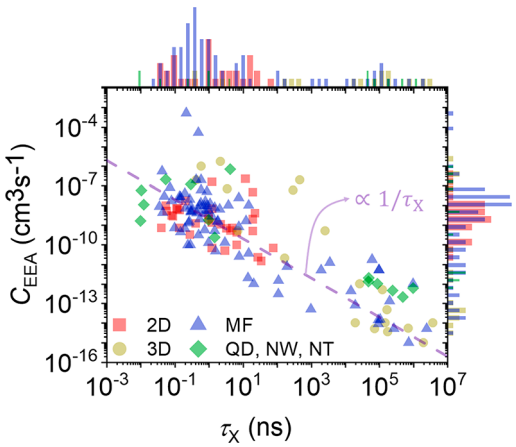

Figure 2. Exciton−exciton annihilation coefficient vs exciton lifetime. Exciton−exciton annihilation coefficient decreases with increasing single exciton lifetime in different excitonic materials. 2D, MF, 3D, QD, NW, and NT are abbreviations of two-dimensional, molecular films, three-dimensional, quantum dot, nanowire, and nanotube, respectively. The relative histogram of C_{EEA} and τ_X is shown on right and top, respectively and has the same color coding as the main figure. Each decade is divided into two bins; the height of the bars represents how many values fall into each interval. The bars on the histogram have different widths for distinguishability; it carries no numerical significance.

We now present a quantum theory of interacting dipoles that provides an intuitive understanding of the crucial mechanism that leads to the inverse relationship between EEA coefficient and single-exciton lifetime. We first explore the microscopic EEA rate at the limit where excitons do not diffuse. Then we introduce exciton diffusion and relate the macroscopic EEA coefficient C_{EEA} with the microscopic rate. Let us consider the nonradiative transfer of energy from a donor exciton to an acceptor exciton that are very close to each other and fixed at nearby sites, as shown in Figure 3. This is similar to fluorescence resonance energy transfer (FRET); however, unlike FRET, the acceptor site is at an excited state. Energy levels that are relevant to exciton−exciton annihilation (EEA) are also shown in Figure 3. The ground-state (a), the first excited-state (b), and higher excited-state (c) energies of a pair of excitons are labeled. These energy levels could be the discrete levels of Frenkel excitons discussed in Figure 1A or relevant k-states of Wannier−Mott excitons in Figure 1B. At the beginning, both donor and acceptor excitons are in their ground excited state, b. After EEA, the donor exciton is annihilated, and the acceptor is excited to higher energy state c. If the wave functions are denoted by ψ, the initial and final state can be written as $|\psi_b^A\ \psi_b^D\rangle$ and $|\psi_c^A\ \psi_a^D\rangle$, respectively. Therefore, from Fermi's golden rule, the rate of nonradiative energy transfer can be written as

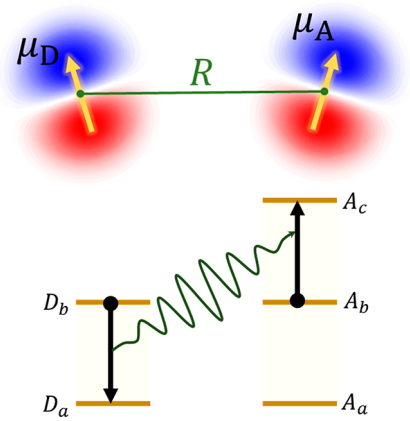

Figure 3. Interaction between excitons. Nonradiative energy transfer between two excitons either in molecular systems or crystalline semiconductors. The transition rate depends on the relative orientation of the transition dipole moments and the distance R between them.

$$B = \frac{2\pi}{\hbar}|\langle\psi_c^A\psi_a^D|V|\psi_b^A\psi_b^D\rangle|^2\rho_F$$

where V is the dipole−dipole interaction potential and ρ_F is the density of states at the energy of the final states. The electrostatic potential between two dipoles that have transition dipole moments of μ_A and μ_D and are distance R apart can be approximated as

$$V \propto \frac{\mu_A\mu_D}{R^3}$$

where angular dependence is ignored for simplicity. Substituting the potential on the rate equation and using the fact that the coordinates of donor and acceptor excitons are independent, we can write

https://dx.doi.org/10.1021/acs.nanolett.0c03820
Nano Lett. XXXX, XXX, XXX−XXX

$$B \propto \frac{1}{R^6} |\langle \psi_a^D | \mu_D | \psi_b^D \rangle|^2 |\langle \psi_c^A | \mu_A | \psi_b^A \rangle|^2$$

The first matrix element of the product is proportional to the rate of transition of the donor exciton to the ground state, independent of the presence of any other excitons, which is inversely related to the single exciton lifetime (τ_X). The second matrix element of the product is proportional to the rate of transition of the acceptor exciton to a higher excited state, which is related to the relative absorptivity of these two levels and is independent of the single exciton lifetime (τ_X). Therefore, the microscopic EEA coefficient, B ,is inversely proportional to τ_X, $\left(B \propto \frac{1}{\tau_X}\right)$.

Now let us consider the case where the excitons can move on a lattice of points in a crystal or among molecules in a film, denoted by a vector $\mathbf{q}$ that has the same dimensionality as the material. The time evolution of the probability $f_q(t)$ of finding an exciton at point q can be written as[12−14]

$$\frac{df_q(t)}{dt} = \frac{f_q(t)}{\tau_X} + F\left[\sum_{q',q'\neq q} f_{q'}(t) - f_q(t)\right] - \int_0^t dt' \Gamma(t-t') f_q^2(t') \quad (4)$$

where F is the rate of diffusion between two adjacent points and $\Gamma(t)$ is a memory function that takes into account of the movement of excitons prior to annihilation and depends on both the microscopic EEA coefficient B and the diffusion rate F. Dividing the probabilities with unit cell volume V gives us the mean-field rate equation[15] stated in eq 1. The diffusion coefficient D is related to the diffusion rate as $D = FA$, where A is the average unit-cell side area. The macroscopic EEA rate coefficient C_{EEA} results from the integration of the memory function term on eq 1. Detail derivation of the memory function gives the following expression in one dimension[16]

$$C_{EEA} = V\frac{B\sqrt{1+4F\tau_X}}{B\tau_X + \sqrt{1+4F\tau_X}}$$

relating macroscopic EEA rate coefficient C_{EEA} to the microscopic EEA rate and diffusion coefficient. We have already derived that $B \propto 1/\tau_X$, therefore

$$C_{EEA} \propto \frac{1}{\tau_X}\frac{\sqrt{1+4F\tau_X}}{B\tau_X + \sqrt{1+4F\tau_X}} \quad (5)$$

In an excitonic semiconductor, two limiting cases of transport are often distinguished.[1,17] In hopping transport, the Frenkel exciton is almost localized, and they can transfer from one site to another. In molecular crystals where hopping is the main mechanism of diffusion, it is known from the Smoluchowski−Einstein theory of random walks that[18−21]

$$F \propto \frac{1}{\tau_X}$$

Therefore, from eq 5, for hopping-dominated diffusion, we get $C_{EEA} \propto \frac{1}{\tau_X}$.

In band transport, phonons scatter the Wannier−Mott excitons in a crystalline semiconductor from one wavevector state to another. The transport is then governed by the scattering times of the wavevector states. The dependence of diffusion constant on the exciton lifetime at the band limit is complex but it decreases with increasing lifetime.[22,23] Combination of these relationships still leads to decreasing C_{EEA} with increasing τ_X. If the diffusion rate is large $(\sqrt{1+4F\tau_X} \gg B\tau_X)$ then also $C_{EEA} \propto \frac{1}{\tau_X}$ Therefore, for both types of transport, we observe decreasing EEA coefficient with increasing lifetime. The relationship between macroscopic and microscopic EEA coefficients are convoluted in higher dimensions, but in all dimensions, C_{EEA} decreases with increasing exciton lifetime.[12,14]

The onset exciton density and recombination rate at which relative quantum yield drops to half of the low pump value can be written as

$$n_{1/2} = \frac{1}{C_{EEA}\tau_X}, \; G_{1/2} = \frac{2}{C_{EEA}\tau_X^2} \quad (6)$$

Both quantities have a more direct impact on practical applications than either lifetime or EEA coefficient. For light-emitting devices, higher onset recombination rate $G_{1/2}$ would imply higher photon emission rate without dropping efficiency due to EEA. In the case of Bose−Einstein condensation or excitonic lasing, larger onset exciton concentration $n_{1/2}$ would imply a large number of quasiparticles can be amassed in that material without sacrificing lifetime. We show $G_{1/2}$ and $n_{1/2}$ in Figure 4 as a function of τ_X in different materials. If C_{EEA} and τ_X were independent, eq 6 would suggest that $G_{1/2}$ is inversely proportional to τ_X^2. However, as a consequence of the trend

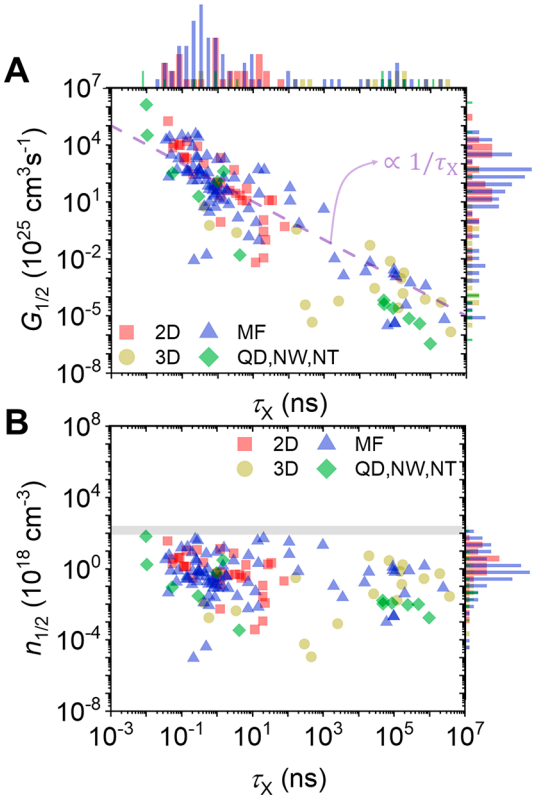

Figure 4. Onset of exciton−exciton annihilation. (A) Generation rate and (B) exciton concentration at the onset of exciton−exciton annihilation. 2D, MF, 3D, QD, NW, and NT are abbreviations of two-dimensional, molecular films, three-dimensional, quantum dot, nanowire, and nanotube, respectively. Histograms of onset generation rate and exciton concentration are shown on the left.

https://dx.doi.org/10.1021/acs.nanolett.0c03820
Nano Lett. XXXX, XXX, XXX−XXX

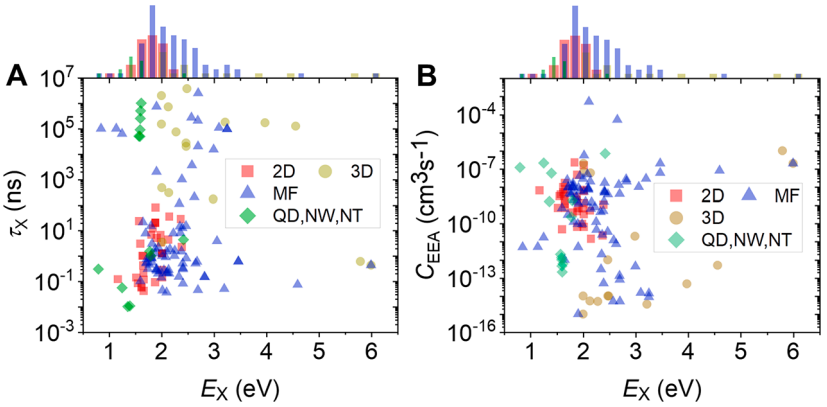

Figure 5. EEA coefficient and exciton lifetime with exciton transition energy. (A) EEA coefficient and (B) single exciton lifetime as a function of exciton emission energy E_X. 2D, MF, 3D, QD, NW, and NT are abbreviations of two-dimensional, molecular films, three-dimensional, quantum dot, nanowire, and nanotube, respectively. Relative histogram of exciton transition energy is shown on the top.

between EEA coefficient and lifetime, $G_{1/2}$ scales inversely with τ_X, independent of the type of exciton, material or diffusion involved (Figure 4A). Therefore, materials with very short lifetimes such as 2D semiconductors are suitable for bright light-emitting devices. Because materials with short lifetimes have the largest $C_{EEA,}$ materials with the largest C_{EEA} also has the largest onset recombination rate for EEA.

$$C_{EEA} \propto \frac{1}{\tau_X} \rightarrow G_{1/2} = \frac{2}{C_{EEA}\tau_X^2} \propto C_{EEA}$$

Similarly, if C_{EEA} and τ_X were independent, eq 6 would suggest that $n_{/2}$ is inversely proportional to τ_X. However, because of the inverse scaling of EEA coefficient with lifetime, onset exciton concentration shows no strong dependence on τ_X (Figure 4B). In all excitonic materials characterized in the literature, EEA begins to dominate the recombination process below an exciton concentration of 1×10^{20} cm^{-3}, corresponding to an interexciton distance of just 2.7 nm. This is a very important number to gauge the potential of future excitonic materials compared to the existing library of materials. The inverse scaling of EEA coefficient with single-exciton lifetime leads to strikingly different scaling of onset recombination rate and onset exciton concentration with lifetime, which is not evident from eq 6. We also show the EEA coefficient and lifetime with corresponding exciton emission energy for different materials in Figure 5. We do not observe any general correlation among them. Optical bandgap of 90% of the materials, in which EEA has been characterized, lies between 1.5 to 2.5 eV.

At high densities, EEA dominates the efficiency and performance of any application of excitonic materials. Our analysis demonstrates the inverse scaling of EEA coefficient with lifetime and elaborates on the enormous role this trend plays in shaping the practically important performance metrics such as onset exciton concentration across different material systems. It is remarkable that despite the broad differences in the material systems examined here, their photophysical parameters exhibit similar qualitative and quantitative pattern. This common structure arises from the underlying fundamental physics of excitons. The photophysics of nanoscale materials is governed by excitons.[1] As more new optical nanomaterials are synthesized in the future, this work will serve as a point of reference to benchmark them and assess their rank in the library of excitonic materials for optoelectronic applications. The macroscopic understanding EEA also enables the estimation of EEA coefficient from lifetime and vice versa for new materials. The insight that recombination rate at the onset of EEA is linearly correlated to EEA coefficient is paradigm shifting. The upper limit of 1×10^{20} cm^{-3} for onset exciton concentration found here is a key design constraint for optoelectronic devices and quasiparticle experiments. Finally, we note that the pattern uncovered here could be a subset of other unifying characteristics in different nanoscale systems that arises from their excitonic nature and further studies in this direction will improve fundamental understanding of material-independent excitonic characteristics.

■ ASSOCIATED CONTENT

Supporting Information

The Supporting Information is available free of charge at https://pubs.acs.org/doi/10.1021/acs.nanolett.0c03820.

EEA coefficient and exciton lifetime of all the different materials used in this work are presented in Table S1 along with their references (PDF)

■ AUTHOR INFORMATION

Corresponding Author

Ali Javey − *Electrical Engineering and Computer Sciences, University of California, Berkeley, Berkeley, California 94720, United States; Materials Sciences Division, Lawrence Berkeley National Laboratory, Berkeley, California 94720, United States;* orcid.org/0000-0001-7214-7931; Email: ajavey@berkeley.edu

Authors

Shiekh Zia Uddin − *Electrical Engineering and Computer Sciences, University of California, Berkeley, Berkeley, California 94720, United States; Materials Sciences Division, Lawrence Berkeley National Laboratory, Berkeley, California 94720, United States;* orcid.org/0000-0002-1265-9940

Eran Rabani − *Materials Sciences Division, Lawrence Berkeley National Laboratory, Berkeley, California 94720, United States; Department of Chemistry, University of California, Berkeley, Berkeley, California 94720, United States; The Raymond and Beverly Sackler Center of Computational Molecular and Materials Science, Tel Aviv University, Tel Aviv 69978, Israel;* orcid.org/0000-0003-2031-3525

Complete contact information is available at:

https://dx.doi.org/10.1021/acs.nanolett.0c03820
Nano Lett. XXXX, XXX, XXX−XXX

https://pubs.acs.org/10.1021/acs.nanolett.0c03820

Author Contributions

S.Z.U. and A.J. conceived the idea for the project. All authors analyzed the data, performed theoretical modeling, wrote and commented on the manuscript.

Notes

The authors declare no competing financial interest.

■ ACKNOWLEDGMENTS

Modelling and simulations were funded by the University of California Multicampus-National Laboratory Collaborative Research and Training program (LFRP-17-477237). PL QY measurements of some of the materials were supported by the U.S. Department of Energy, Office of Science, Office of Basic Energy Sciences, Materials Sciences and Engineering Division, under contract DE-AC02-05CH11231 within the Electronic Materials Program (KC1201).

■ REFERENCES

(1) Scholes, G. D.; Rumbles, G. Excitons in Nanoscale Systems. *Nat. Mater.* **2006**, *5*, 683−696.
(2) Davydov, A. S. The Theory of Molecular Excitons. *Phys.-Uspekhi* **1964**, *7* (2), 145.
(3) Brus, L. Zero-dimensional Excitons in Semiconductor Clusters. *IEEE J. Quantum Electron.* **1986**, *22* (9), 1909−1914.
(4) Wang, F.; Dukovic, G.; Brus, L. E.; Heinz, T. F. The Optical Resonances in Carbon Nanotubes Arise from Excitons. *Science* **2005**, *308* (5723), 838−841.
(5) Splendiani, A.; Sun, L.; Zhang, Y.; Li, T.; Kim, J.; Chim, C. Y.; Galli, G.; Wang, F. Emerging Photoluminescence in Monolayer MoS_2. *Nano Lett.* **2010**, *10* (4), 1271−1275.
(6) Koch, S. W.; Kira, M.; Khitrova, G.; Gibbs, H. M. Semiconductor Excitons in New Light. *Nat. Mater.* **2006**, *5* (7), 523−531.
(7) Adachi, C.; Baldo, M. A.; Thompson, M. E.; Forrest, S. R. Nearly 100% Internal Phosphorescence Efficiency in an Organic Light-emitting Device. *J. Appl. Phys.* **2001**, *90* (10), 5048−5051.
(8) Suna, A. Kinematics of Exciton-exciton Annihilation in Molecular Crystals. *Phys. Rev. B* **1970**, *1* (4), 1716.
(9) May, V. Kinetic Theory of Exciton-exciton Annihilation. *J. Chem. Phys.* **2014**, *140* (5), 054103.
(10) Nguyen, D. T.; Voisin, C.; Roussignol, P.; Roquelet, C.; Lauret, J. S.; Cassabois, G. Elastic Exciton-exciton Scattering in Photoexcited Carbon Nanotubes. *Phys. Rev. Lett.* **2011**, *107* (12), 127401.
(11) Lien, D. H.; Uddin, S. Z.; Yeh, M.; Amani, M.; Kim, H.; Ager, J. W.; Yablonovitch, E.; Javey, A. Electrical Suppression of All Nonradiative Recombination Pathways in Monolayer Semiconductors. *Science* **2019**, *364* (6439), 468−471.
(12) Kenkre, V. M. Validity of the Bilinear Rate Equation for Exciton Annihilation and Expressions for the Annihilation Constant. *Z. Phys. B: Condens. Matter Quanta* **1981**, *43* (3), 221−227.
(13) Wang, L.; May, V. Theory of Multiexciton Dynamics in Molecular Chains. *Phys. Rev. B: Condens. Matter Mater. Phys.* **2016**, *94* (19), 195413.
(14) Katsch, F.; Selig, M.; Carmele, A.; Knorr, A. Theory of Exciton-exciton Interactions in Monolayer Transition Metal Dichalcogenides. *Phys. Status Solidi B* **2018**, *255* (12), 1800185.
(15) Reineker, P. *Exciton Dynamics in Molecular Crystals and Aggregates*; Springer: Berlin, 1982; Vol. *94*.
(16) Kenkre, V. M. Theory of Exciton Annihilation in Molecular Crystals. *Phys. Rev. B: Condens. Matter Mater. Phys.* **1980**, *22* (4), 2089.
(17) Munn, R. W.; Silbey, R. Remarks on Exciton-Phonon Coupling and Exciton Transport. *Mol. Cryst. Liq. Cryst.* **1980**, *57* (1), 131−144.
(18) Freund, J. A.; Pöschel, T. *Stochastic Processes in Physics, Chemistry, and Biology*; Springer Science & Business Media: Berlin, 2000; Vol. *557*.
(19) Mikhnenko, V. O.; Blom, P. W.; Nguyen, T.-Q. Exciton Diffusion in Organic Semiconductors. *Energy Environ. Sci.* **2015**, *8* (7), 1867−1888.
(20) Madigan, C.; Bulović, V. Modeling of Exciton Diffusion in Amorphous Organic Thin Films. *Phys. Rev. Lett.* **2006**, *96* (4), 046404.
(21) Fennel, F.; Lochbrunner, S. Exciton-exciton Annihilation in a Disordered Molecular System by Direct and Multistep Förster Transfer. *Phys. Rev. B: Condens. Matter Mater. Phys.* **2015**, *92* (14), 140301.
(22) Erland, J.; Razbirin, B. S.; Pantke, K. H.; Lyssenko, V. G.; Hvam, J. M. Exciton Diffusion in CdSe. *Phys. Rev. B: Condens. Matter Mater. Phys.* **1993**, *47* (7), 3582.
(23) Čápek, V.; Munn, R. W. Exciton Transport in the Band Limit. *J. Chem. Phys.* **1982**, *76* (9), 4674−4675.

https://dx.doi.org/10.1021/acs.nanolett.0c03820
Nano Lett. XXXX, XXX, XXX−XXX